08

Features of $SnO_2/Ga_2O_3/GaN/Al_2O_3$ Multilayer Film Domain Structure

© M.E. Boiko[1], M.D. Sharkov[1], A.M. Boiko[1], P.N. Butenko[1], A.V. Almaev[2], V.I. Nikolaev[1]

[1] Ioffe Institute, St. Petersburg, Russia
[2] Tomsk State University, Tomsk, Russia
E-mail: boikomix@gmail.com, mischar@mail.ru

Received June 11, 2024
Revised August 20, 2024
Accepted August 21, 2024

In a film $SnO_2/Ga_2O_3/GaN/Al_2O_3$ grown via vapor-phase epitaxial techniques a study of domains formation has been performed with the help of X-ray diffraction. The estimations of domain sizes in the film normal direction within film layers and the substrate have been obtained. Reduction of crystal perfectness in layers along their remoteness from the substrate has been stated. The hypothesis of amorphous or nanosized structure of the upside tin dioxide layer has been formulated

Keywords: Semiconductor Heterostructures, Multilayer Films, X-Ray Diffraction, Domain Structure, Crystal Perfectness.

DOI: 10.61011/TPL.2025.01.60132.20018

The interest in semiconductor heterostructures based on gallium oxide (Ga_2O_3) [1,2] and tin dioxide (SnO_2) [3,4] has been on the rise lately. Ga_2O_3 is a polymorphic compound with the monoclinic β-phase being the most stable [1]: group $C2/m$ (No. 12), $a = 12.227$ Å, $b = 3.0389$ Å, $c = 5.8079$ Å, and $\beta = 103.82°$ (card 00-041-1103 from the ICDD database). β-Ga_2O_3 is a semiconductor with a band gap of 4.9 eV [1,2]. One other Ga_2O_3 modification worthy of mention is the κ-phase, which is also known as the ε-phase [1,5,6]: orthorhombic, group $Pna2_1$ (No. 33), $a = 5.0463$ Å, $b = 8.7020$ Å, and $c = 9.2833$ Å [5].

SnO_2 has various applications in physics and chemistry (e.g., in solar cells [3] and gas analyzers [4,7]). Just as Ga_2O_3, this material is characterized by polymorphism, which is manifested mainly at high pressures (in most cases, above 100 kbar) [4,8]. The primary phase of SnO_2 is a tetragonal structure of the rutile type with symmetry group $P4_2/mnm$ (No. 136) [9] with lattice parameters $a = 4.7382$ Åand $c = 3.1871$ Å. Similar to β-gallium oxide, SnO_2 is a wide-gap semiconductor with a band gap of approximately 3.6 eV [4].

In turn, gallium nitride (GaN) is also a wide-bandgap semiconductor with a similar band gap width: 3.5–3.6 eV [10]. It is characterized by a hexagonal lattice of the $P6_3mc$ group (No. 186) with parameters $a = 3.190$ Åand $c = 5.189$ Å (ICDD card 01-070-2546).

Both the β-phase of Ga_2O_3 [11,12] and SnO_2 [13] are semiconductors in which p-type conductivity is hard to implement. In the case of gallium oxide, it was proposed in [14] to establish hole conductivity in β-Ga_2O_3 by transforming GaN into β-Ga_2O_3 via crystal-chemical oxidation of nitride. Thus, a grown $SnO_2/Ga_2O_3/GaN$ film is a semiconductor heterostructure with restrictions on doping, where the SnO_2 layer is likely to remain n-type and the layer of Ga_2O_3 (a semiconductor that normally allows only n-type doping [11,12]) may contain holes with a concentration around $3 \cdot 10^{15}\,\mathrm{cm}^{-3}$ [14]. Such a material is of potential interest as a new heterostructure in which one of the layers may have an atypical conductivity type.

When a $Ga_2O_3/GaN/Al_2O_3$ structure is grown, the upper oxide layer may form in both the β-phase [15] and the κ-one [16], and the latter was confirmed in experiments carried out by some of the authors of the present study [17,18]. In turn, the authors of [19] have demonstrated the possibility of formation of both modifications (β- and $\kappa(\varepsilon)$-Ga_2O_3) on a GaN (0001)/α-Al_2O_3 (0001) surface. As was noted in [19], the β-phase and the κ-phase grow in directions $[\bar{2}01]$ and [001], respectively.

At the initial stage of formation of the $SnO_2/Ga_2O_3/GaN/\alpha$-Al_2O_3 film studied here and earlier in [7], a GaN layer with a thickness of 3 μm was grown on a single-crystal α-Al_2O_3 substrate by metal-organic chemical vapor deposition (MOCVD) at a temperature of approximately 1350 K. The next layer of Ga_2O_3 1 μm in thickness was grown on the nitride layer by halide vapor phase epitaxy (HVPE) at a temperature of approximately 900 K. At the final stage, a 120-nm-thick SnO_2 film was deposited by magnetron sputtering of a Sn target in oxygen–argon plasma (with 56% of oxygen) at room temperature in a rarefied environment (7 μbar). Upon completion of growth procedures, the film was annealed in air at a temperature about 900 K for 4 h.

The data from [7] confirm the presence of a significant fraction of Sn in the sample: this follows from the examination of photoemission lines corresponding to the M_{IV}-edge and the M_V-edge of Sn and from the band gap measurement results (3.76 eV for the surface layer, which is close to the data for SnO_2). A qualitative phase analysis of X-ray diffraction data was also carried out in [7]. It revealed the presence of α-Al_2O_3, GaN, and one of the Ga_2O_3 phases (β- or $\kappa(\varepsilon)$-phase) in the sample. In the present study, the X-ray diffraction patterns are subjected to

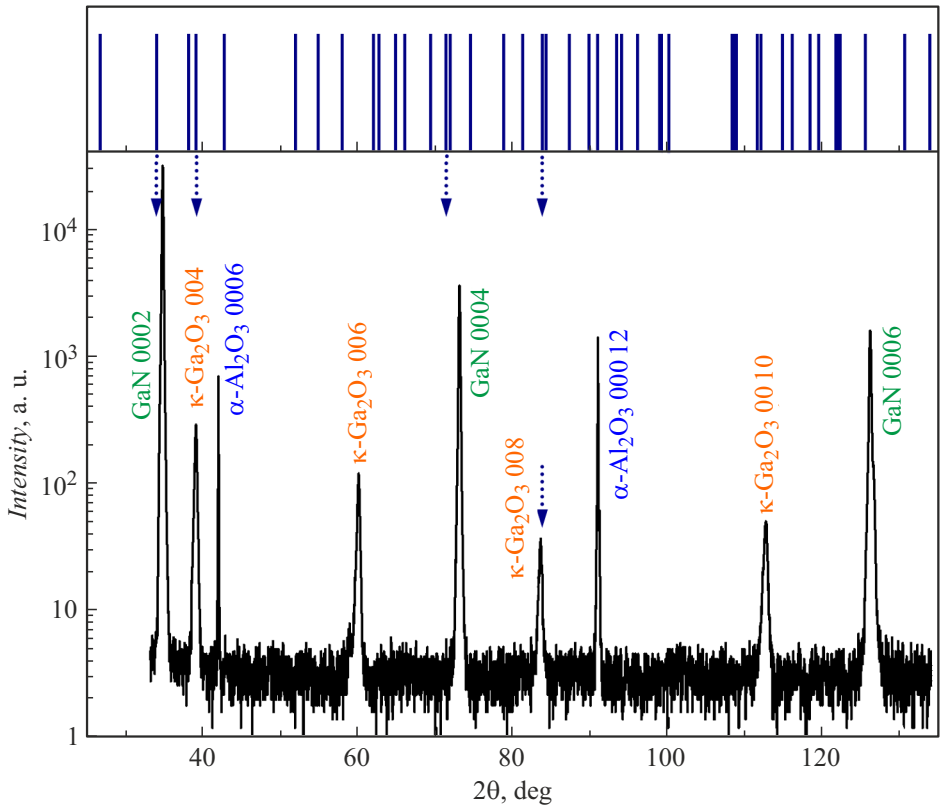

XRD data for the examined $SnO_2/Ga_2O_3/GaN/Al_2O_3$ sample. Positions of SnO_2 reflections taken from [9] are indicated above. Dotted arrows denote the SnO_2 reflections: 101, 111, 202, and 222 (in the order of increasing scattering angles).

a more thorough examination, which includes processing of the reflection shape and a more accurate determination of interplanar distances in the sample components.

X-ray diffraction (XRD) curves were measured using a DRON-7 laboratory diffractometer (Ioffe Institute) with an extended base in the quasi-parallel mode with an SCSD-4C scintillation detector and a Ge (111) monochromator crystal under monochromatic Cu$K_{\alpha 1}$- irradiation (1.5406 Å). The diffraction curve for the examined sample is shown in the figure. It features several series of reflections, each corresponding to the crystallographic direction along the normal to the film and one of its layers. The figure also shows the bar diagram of SnO_2 reflections (they are shown as dotted arrows of the same length, since the ICDD data correspond to powder samples that have neither a preferred orientation nor textural distortions). The list of reflections and their probable identification are presented in the table.

First, two narrowest reflections located around 2θ angles of approximately 41.71 and 90.76° are observed. They correspond to reflections 0006 and 000 12 of α-Al_2O_3 (41.67 and 90.69° in the ICDD 01-077-2135 card, respectively), yield an interplanar distance of 2.165 Å (2.166 Åin ICDD 01-077-2135), and serve as an internal reference for XRD studies. Second, the reflections at 34.52, 72.87, and 125.95° correspond to reflections 0002, 0004, and 0006 of GaN and yield an interplanar distance of 2.594 Å (34.54, 72.85, 125.91°, and 2.5945 Åin the ICDD 01-070-2546 card, respectively).

The recorded XRD curve also features a series of reflections in the vicinity of angles 38.82, 59.83, 83.38, and 112.46°. This series may correspond to one of the phases of gallium oxide: β-Ga_2O_3 or $\kappa(\varepsilon)$-Ga_2O_3. In the former case, these are reflections $\bar{4}02$, $\bar{6}03$, $\bar{8}04$, and $\overline{10}$ 05; in the latter case, these are reflections 004, 006, 008, and 00 10. It follows from the table that such maxima positions are more fitting for the κ-phase. The tabular interplanar distances in matrices β- and $\kappa(\varepsilon)$-Ga_2O_3 (β-Ga_2O_3 $\bar{2}01$ and $\kappa(\varepsilon)$-Ga_2O_3 002) are 4.68–4.69 Åfor β-Ga_2O_3 (cards ICDD 00-041-1103, 01-074-1776, and 01-087-1901) and approximately 4.642 Å [5] and 4.633 Å(this study) for $\kappa(\varepsilon)$-Ga_2O_3.

Reflections potentially corresponding to other directions of Al_2O_3 (substrate), GaN, and β- or $\kappa(\varepsilon)$-Ga_2O_3 (two lower layers) were not found in the diffraction pattern shown in the figure. It follows that the substrate and two lower layers of the sample are single crystals or mosaics of coherent (quasi-coherent) domains.

SnO_2 reflections could potentially be present in the diffraction pattern. For example, reflection SnO_2 101 is fairly close to GaN 0002, although SnO_2 202 is quite far (the approximate distance is 1.5°) from GaN 0004. Reflections SnO_2 111 and SnO_2 222 are close (with probable distortion caused by epitaxial growth processes

Reflections from the $SnO_2/Ga_2O_3/GaN/Al_2O_3$ sample and their identification (either a card number in the ICDD database or a literature reference is given in the „Source“ column)

Angle 2θ, deg	Probable reflection	Angle 2θ for the reflection, deg	Source
34.52	SnO_2 101 GaN 0002	33.87 34.54	[9] 01-070-2546
38.82	β-Ga_2O_3 $\bar{4}02$ $\kappa(\varepsilon)$-Ga_2O_3 004 SnO_2 111	38.45 38.77 38.97	01-074-1776 [5] [9]
41.71	Al_2O_3 0006	41.67	01-077-2135
59.83	β-Ga_2O_3 $\bar{6}03$ $\kappa(\varepsilon)$-Ga_2O_3 006	59.19 59.72	01-074-1776 [5]
72.87	SnO_2 202 GaN 0004	71.26 72.85	[9] 01-070-2546
83.38	β-Ga_2O_3 $\bar{8}04$ $\kappa(\varepsilon)$-Ga_2O_3 008 SnO_2 222	82.37 83.18 83.69	01-074-1776 [5] [9]
90.76	Al_2O_3 000 12	90.69	01-077-2135
112.46	β-Ga_2O_3 $\overline{10}$ 05 $\kappa(\varepsilon)$-Ga_2O_3 00 10	110.80 112.15	01-074-1776 [5]
125.95	$SnO_2$303 GaN 0006	121.81 125.91	[9] 01-070-2546

factored in) to reflections $\kappa(\varepsilon)$-Ga_2O_3 004 and $\kappa(\varepsilon)$-Ga_2O_3 008, respectively.

It follows from the analysis of profiles of reflection curves from the substrate and grown layers that the full width at half-maximum (FWHM) of the substrate peaks should be approximately an order of magnitude smaller than the one corresponding to reflections from the epitaxial layers. In the present case,

$\mathrm{FWHM}(Al_2O_3\ 0006) = 2.8\,\mathrm{arcmin}$,

$\mathrm{FWHM}(\mathrm{GaN}\ 0002) = 10.5\,\mathrm{arcmin}$,

$\mathrm{FWHM}(\kappa(\varepsilon)\text{-}Ga_2O_3\ 006) = 14.3\,\mathrm{arcmin}$.

Having processed the XRD curve using the Scherrer's and Williamson–Hall methods [20], we obtained approximate estimates of 210, 50, and 30 nm for the corresponding coherent scattering regions (CSRs). A reduction in domain sizes in the direction normal to the film is actually observed as one moves from the substrate to the film surface.

The FWHM of the first reflection for the $\kappa(\varepsilon)$-Ga_2O_3 layer in the figure is approximately a third larger than the corresponding value for the GaN intermediate layer and 5 times larger than for the Al_2O_3 substrate (14.3, 10.5, and 2.8 arcmin, respectively). In addition, the intensity of substrate reflections is suppressed by the mass absorption of epitaxial layers. It is important to note that the second layer (gallium oxide) produces reflections that are approximately two orders of magnitude weaker than those of the underlying nitride layer. This is a further illustration of the significantly lower degree of perfection of the gallium oxide layer. This suggests that the upper layer of tin dioxide grown on a low-quality surface (compared to the substrate and the bottom layer) is characterized by an even lower degree of perfection, and the CSR for the upper layer is even smaller (at the level of a finely dispersed crystal). Weak broadened peaks of SnO_2 overlapping with the reflections of $\kappa(\varepsilon)$-Ga_2O_3 then remain unresolved in our experiments.

Thus, it was demonstrated that the second layer is characterized by a lower degree of perfection and does not facilitate the formation of a subsequent layer of high crystallinity on its surface. The XRD pattern suggests that the upper layer of tin dioxide is amorphous or forms a finely dispersed crystalline phase.

Conflict of interest

The authors declare that they have no conflict of interest.

References

[1] S.I. Stepanov, V.I. Nikolaev, V.E. Bougrov, A.E. Romanov, Rev. Adv. Mater. Sci., **44** (1), 63 (2016). http://www.ipme.ru/e-journals/RAMS/no_14416/06_14416_stepanov.pdf

[2] N.S. Jamwal, A. Kiani, Nanomaterials, **12** (12), 2061 (2022). DOI: 10.3390/nano12122061

[3] A. Uddin, H. Yi, Solar RRL, **6** (6), 2100983 (2022). DOI: 10.1002/solr.202100983

[4] S. Das, V. Jayaraman, Prog. Mater. Sci., **66**, 112 (2014). DOI: 10.1016/j.pmatsci.2014.06.003
[5] I. Cora, F. Mezzadri, F. Boschi, M. Bosi, M. Čaplovičová, G. Calestani, I. Dódony, B. Pécz, R. Fornari, CrystEngComm, **19** (11), 1509 (2017). DOI: 10.1039/c7ce00123a
[6] S. Yusa, D. Oka, T. Fukumura, CrystEngComm, **22** (2), 381 (2019). DOI: 10.1039/c9ce01532a
[7] A. Almaev, N. Yakovlev, V. Kopyev, V. Nikolaev, P. Butenko, J. Deng, A. Pechnikov, P. Korusenko, A. Koroleva, E. Zhizhin, Chemosensors, **11** (6), 325 (2023). DOI: 10.3390/chemosensors11060325
[8] K.M.O. Jensen, M. Christensen, P. Juhas, C. Tyrsted, E.D. Bojesen, N. Lock, S.J.L. Billinge, B.B. Iversen, J. Am. Chem. Soc., **134** (15), 6785 (2012). DOI: 10.1021/ja300978f
[9] T. Yamanaka, R. Kurashima, J. Mimaki, Z. Kristallogr., **215** (7), 424 (2000). DOI: 10.1524/zkri.2000.215.7.419
[10] Y.-N. Xu, W.Y. Ching, Phys. Rev. B, **48** (7), 4335 (1993). DOI: 10.1103/PhysRevB.48.4335
[11] J.B. Varley, J.R. Weber, A. Janotti, C.G. Van de Walle, Appl. Phys. Lett., **97** (14), 142106 (2010). DOI: 10.1063/1.3499306
[12] M. Higashiwaki, K. Sasaki, H. Murakami, Y. Kumagai, A. Koukitu, A. Kuramata, T. Masui, S. Yamakoshi, Semicond. Sci. Technol., **31** (3), 034001 (2016). DOI: 10.1088/0268-1242/31/3/034001
[13] D.O. Scanlon, G.W. Watson, J. Mater. Chem., **22** (48), 25236 (2012). DOI: 10.1039/c2jm34352e
[14] C. Ma, Z. Wu, Z. Jiang, Y. Chen, W. Ruan, H. Zhang, H. Zhu, G. Zhang, J. Kang, T.-Y. Zhang, J. Chu, Z. Fang, J. Mater. Chem. C, **10** (17), 6673 (2022). DOI: 10.1039/d1tc05324h
[15] S.-A. Lee, J.-Y. Hwang, J.-P. Kim, S.-Y. Jeong, C.-R. Cho, Appl. Phys. Lett., **89** (18), 182906 (2006). DOI: 10.1063/1.2374806
[16] T. Chen, X. Zhang, Y. Ma, T. He, X. Wei, W. Tang, W. Tang, X. Zhou, H. Fu, L. Zhang, K. Xu, C. Zeng, Y. Fan, Y. Cai, B. Zhang, Adv. Photon. Res., **2** (8), 2100049 (2021). DOI: 10.1002/adpr.202100049
[17] V.I. Nikolaev, S.I. Stepanov, A.I. Pechnikov, S.V. Shapenkov, M.P. Scheglov, A.V. Chikiryaka, O.F. Vyvenko, ECS J. Solid State Sci. Technol., **9** (4), 045014 (2020). DOI: 10.1149/2162-8777/ab8b4c
[18] S.I. Stepanov, A.I. Pechnikov, M.P. Scheglov, A.V. Chikiryaka, V.I. Nikolaev, Tech. Phys. Lett., **48** (10), 32 (2022). DOI: 10.21883/TPL.2022.10.54794.19169
[19] V. Gottschalch, S. Merker, S. Blaurock, M. Kneiß, U. Teschner, M. Grundmann, H. Krautscheid, J. Cryst. Growth, **510**, 76 (2019). DOI: 10.1016/j.jcrysgro.2019.01.018
[20] V.I. Iveronova, G.P. Revkevich, *Teoriya rasseyaniya rentgenovskikh luchei* (Izd. Mosk. Gos. Univ., M., 1972) (in Russian).

Translated by D.Safin